A novel chaotic system with one source and two saddle-foci in Hopfield neural networks*

Chen Peng-Fei(陈鹏飞)[a)b)†], Chen Zeng-Qiang(陈增强)[a)‡], and Wu Wen-Juan(吴文娟)[a)]

[a)] *Department of Automation, Nankai University, Tianjin* 300071, *China*
[b)] *The Institute of Military Transportation, Tianjin* 300161, *China*

(Received 14 July 2009; revised manuscript received 24 July 2009)

This paper presents the finding of a novel chaotic system with one source and two saddle-foci in a simple three-dimensional (3D) autonomous continuous time Hopfield neural network. In particular, the system with one source and two saddle-foci has a chaotic attractor and a periodic attractor with different initial points, which has rarely been reported in 3D autonomous systems. The complex dynamical behaviours of the system are further investigated by means of a Lyapunov exponent spectrum, phase portraits and bifurcation analysis. By virtue of a result of horseshoe theory in dynamical systems, this paper presents rigorous computer-assisted verifications for the existence of a horseshoe in the system for a certain parameter.

Keywords: Hopfield neural network, chaos, bifurcation, Lyapunov exponents
PACC: 0545

1. Introduction

Since the first remarkable autonomous chaotic system[1] was found by Lorenz in 1963, more and more chaotic phenomena have been found in many research fields. More and more researchers have paid great attention to generating chaos and analysing the dynamics of chaotic systems, such as the Chen system,[2] the Lü system,[3] and so on.[4−11] Moreover, practical applications have given rise to many new and attractive research topics, such as chaos control, chaos synchronization and circuit realization.[12−19] Chaos has been observed in many neural networks, such as discrete time neural networks, time delay neural networks, and continuous neural networks. A Hopfield neural network,[20] abstracted from brain dynamics, is a significant artificial neural network which is able to store certain memories or patterns in a manner rather similar to the brain. Chaos and hyperchaos have been found in autonomous continuous time Hopfield neural networks.[21−26] However, it is not easy to find chaos in three-dimensional (3D) autonomous continuous time Hopfield neural networks.

In this paper we show chaos in the following simplified low dimensional autonomous continuous time Hopfield neural networks:

$$\begin{aligned} & C_i \frac{\mathrm{d}x_i}{\mathrm{d}t} = -\frac{x_i}{R_i} + \sum_{j=1}^{n} w_{ij} v_j + I_i, \\ & i = 1, 2, \ldots, n, \\ & v_i = f_i(x_i), \end{aligned} \tag{1}$$

where f_i is a monotone differentiable function bounded above and below. $W = w_{ij}$ is an $n \times n$ matrix, called a weight matrix or connection matrix describing the strength of connections between neurons.

The organization of the paper is as follows. In Section 2, we present the model of the novel 3D autonomous system and analyse its basic properties. The evolution process analysis, by means of the Lyapunov exponent spectrum, phase portraits and bifurcation analysis, is investigated in Section 3, where detailed numerical simulation studies are given. Furthermore, in Section 4, we give rigorous computer-assisted verifications for the existence of a horseshoe embedded in the chaotic attractor of the system for a certain parameter. Finally, we briefly summarize the results and give a conclusion in Section 5.

*Project supported by the National Natural Science Foundation of China (Grant No. 60774088), the Program for New Century Excellent Talents in University of China (NCET), the Science & Technology Research Key Project of Educational Ministry of China (Grant No. 107024), the Foundation of the Application Base and Frontier Technology Research Project of Tianjin (Grant No. 08JCZDJC21900).
†Corresponding author. E-mail: cpfcare@163.com
‡E-mail: chenzq@nankai.edu.cn
© 2010 Chinese Physical Society and IOP Publishing Ltd

2. System description and its basic properties

In this section, we will study a simplified Hopfield neural network. The dynamic of this system can be described by the following ordinary differential equations:

$$\begin{aligned}&\dot{x}_i = -x_i + \sum_{j=1}^{3} w_{ij} v_j,\\ &i = 1, 2, 3,\\ &v_i = \tanh(x_i) = \frac{\mathrm{e}^{x_i} - \mathrm{e}^{-x_i}}{\mathrm{e}^{x_i} + \mathrm{e}^{-x_i}},\end{aligned} \tag{2}$$

where $W = (w_{ij})$ is a 3×3 matrix, which is

$$W = \begin{bmatrix} w_{11} & w_{12} & w_{13} \\ w_{21} & w_{22} & w_{23} \\ w_{31} & w_{32} & w_{33} \end{bmatrix}, \tag{3}$$

The topological connection of the weight matrix W is illustrated in Fig. 1.

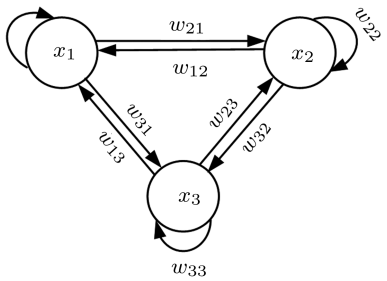


Fig. 1. The topological connection.

It is symmetrical with respect to the origin of coordinate, and $S_1 = (0,\ 0,\ 0)$ is obviously an equilibrium point. Specifically, we consider the following connection matrix:

$$W = \begin{bmatrix} 1 & -6 & 4 \\ p & 3.5 & -1 \\ -1 & 4 & 1.5 \end{bmatrix}, \tag{4}$$

where p is an adjustable parameter. In this paper, we investigate the dynamics of system (2) with the connection matrix (4), and consider the case that the parameter p varies in the range $[1.9,\ 2.4]$.

Linearizing system (2) at the zero equilibrium point S_1 yields the Jacobian matrix:

$$J = \begin{bmatrix} 0 & -6 & 4 \\ p & 2.5 & -1 \\ -1 & 4 & 0.5 \end{bmatrix} \tag{5}$$

and its characteristic equation is

$$\begin{aligned}f(\lambda) &= \lambda^3 - 3\lambda^2 + (9.25 + 6p)\lambda - (4 + 19p)\\ &= 0.\end{aligned} \tag{6}$$

According to the relationship between roots and coefficients of a polynomial, we can prove that all of the roots of Eq. (6) have positive real parts for

$$p \in (-4/19,\ 95/4).$$

That is, the equilibrium S_1 is a source.

The stabilities of the two nonzero equilibria which can be calculated via numerical computation for a certain parameter p will be discussed in the next section.

3. The evolution processes of the new system and bifurcation analysis

In this section, we use the numerical computation and basic bifurcation analysis to investigate the dynamical behaviours of system (2) with the connection matrix (4). As will be shown in the following, the dynamic behaviour of the system is very rich for $p \in [1.9,\ 2.4]$.

When the system evolves with initial point $(1,\ 1,\ 1)$, the Lyapunov exponent spectrum and the corresponding bifurcation diagram of the variable x_1 with respect to p are given in Figs. 2(a) and 2(b) respectively. When the system evolves with initial point $(1,\ -1,\ 1)$, the corresponding bifurcation diagram of the variable x_1 with respect to p are given in Fig. 2(c).

From Figs. 2(a) and 2(b), it can be observed that the bifurcation diagram coincides well with the Lyapunov exponent spectrum. We can find that system (2) with initial point $(1,\ 1,\ 1)$ can be periodic and a chaotic attractor when varying p. But one can find that system (2) with initial point $(1,\ -1,\ 1)$ only has a periodic attractor when varying p from Fig. 2(c). Phase portraits of certain parameters are shown in Fig. 3.

For $p = 1.95$, one limit cycle is found with different initial points, as illustrated in Fig. 3(a).

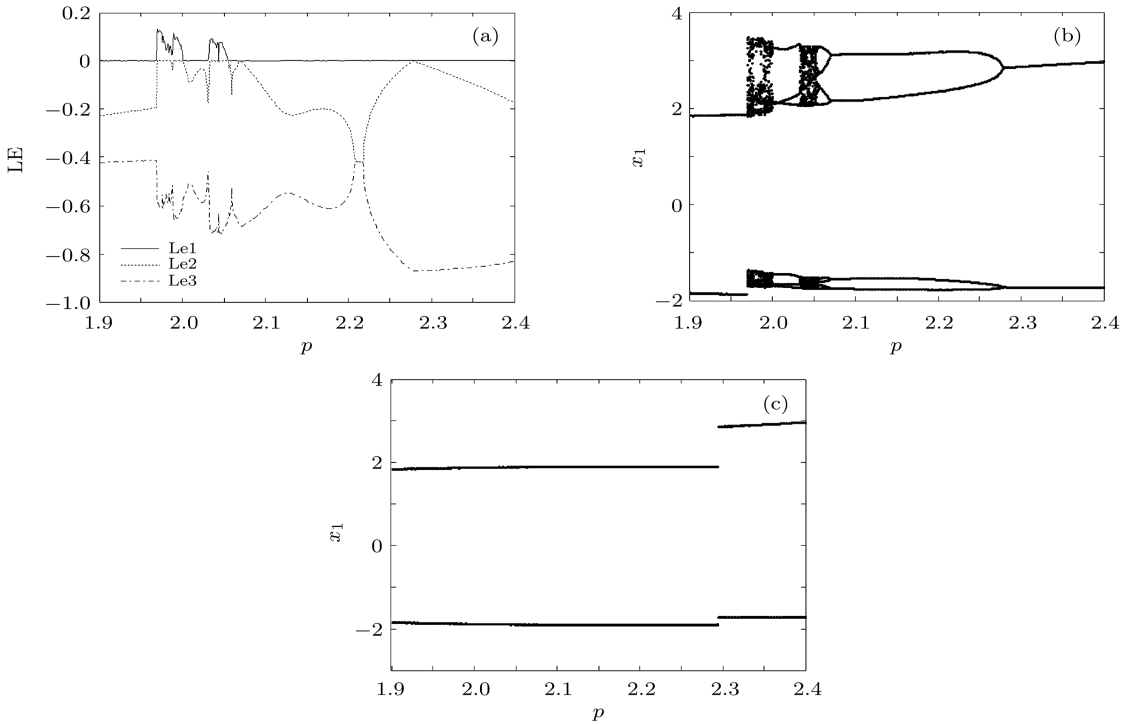


Fig. 2. Lyapunov exponent spectrum and bifurcation diagram vs. p: (a) Lyapunov exponent spectrum with initial point (1, 1, 1); (b) bifurcation diagram of x_1 with initial point (1, 1, 1); (c) bifurcation diagram of x_1 with initial point (1, −1, 1).

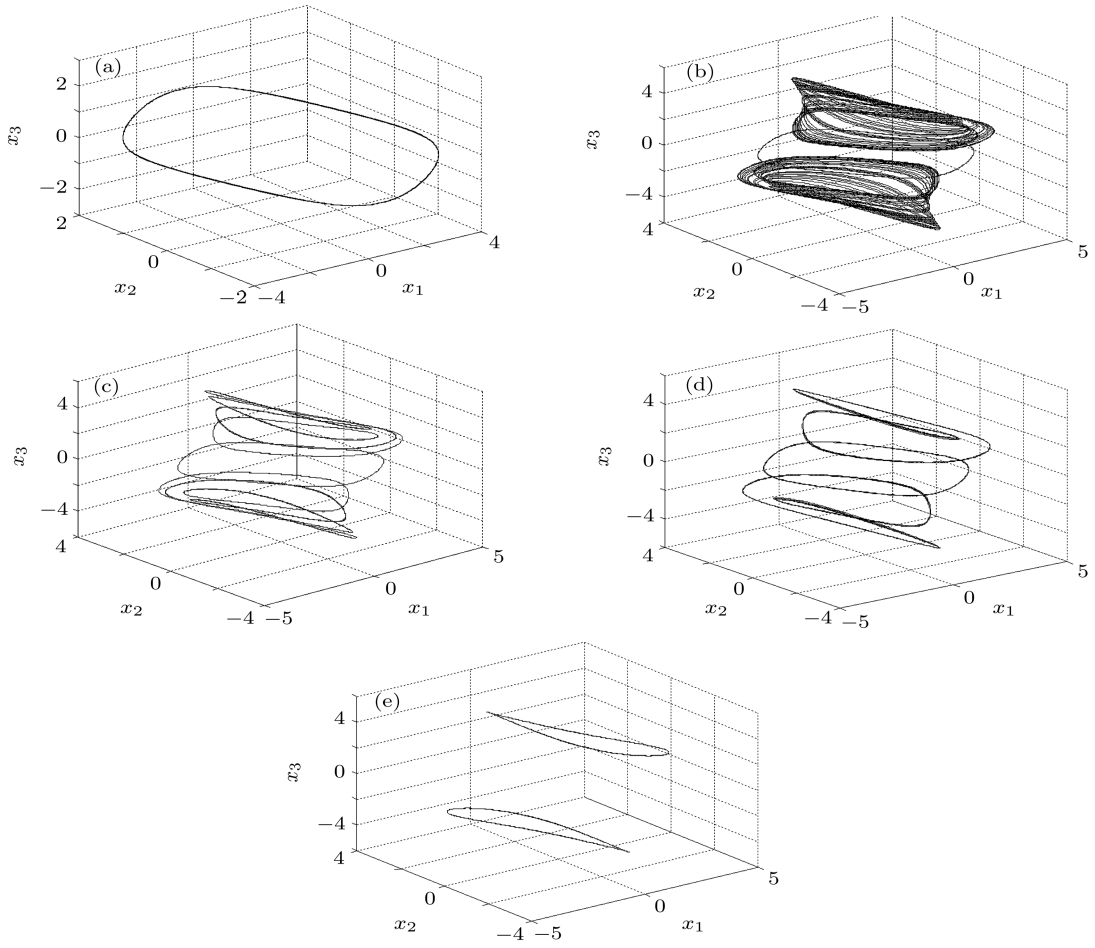


Fig. 3. The phase portraits of system (2) with different parameters p.

For $p = 1.99$, two chaotic attractors illustrated in Fig. 3(b) are found with two different initial points $\pm(1,\ 1,\ 1)$, and one limit cycle is found with initial point $(1,\ -1,\ 1)$. Now the two nonzero equilibria of system (2) are $\pm(-0.2732,\ 0.8064,\ 4.4365)$. Linearizing system (2) at these two equilibria points yields the Jacobian matrix:

$$J = \begin{bmatrix} -0.0711 & -3.3260 & 0.0022 \\ 1.8486 & 0.9402 & -0.0006 \\ -0.9289 & 2.2174 & -0.9992 \end{bmatrix}, \qquad (7)$$

and its characteristic roots are

$$\lambda_{1,2} = 0.4338 \pm 2.4277\mathrm{i}, \quad \lambda_3 = -0.9976.$$

That is, these two equilibria are unstable saddle-foci.

For $p = 2.06$, two period-four limit cycles illustrated in Fig. 3(c) are found with two different initial points $\pm(1,\ 1,\ 1)$, and another limit cycle is found with initial point $(1,\ -1,\ 1)$.

For $p = 2.1$, two period-two limit cycles illustrated in Fig. 3(d) are found with two different initial points $\pm(1,\ 1,\ 1)$, and another limit cycle is found with initial point $(1,\ -1,\ 1)$.

For $p = 2.3$, only two limit cycles illustrated in Fig. 3(e) are found with two different initial points $\pm(1,\ 1,\ 1)$, or with initial points $\pm(1,\ -1,\ 1)$.

Observing the bifurcation diagram and phase portraits, it can be concluded that there exists a period-doubling bifurcation process in system (2) with initial points $(1,\ 1,\ 1)$. Also, the bifurcation point which is just the discontinuity point in Fig. 2(c) is $p = 2.2941$. It is very clear that there remains much to be done from a bifurcation viewpoint.

4. Topological horseshoe

4.1. Review of the topological horseshoe theorem

In this subsection, we recall a result on horseshoe theory developed in Ref. [27], which is essential for the rigorous verification of the existence of chaos in system (2).

Let X be a metric space, D is a compact subset of X, and $f : D \to X$ is a map satisfying the assumption that there exist m mutually disjoint subsets $D_1, \ldots, D_{m-1}$ and D_m of D, the restriction of f to each D_i, i.e. $f|D_i$ is continuous.

Definition 1 Let γ be a compact subset of D, such that for each $1 \le i \le m$, $\gamma_i = \gamma \cap D_i$ is nonempty and compact, then γ is called a connection with respect to $D_1, \ldots, D_{m-1}$ and D_m. Let F be a family of connections γ with respect to $D_1, \ldots, D_{m-1}$ and D_m satisfies the following property:

$$\gamma \in F \Rightarrow f(\gamma_i) \in F.$$

Then F is said to be an f-connected family with respect to $D_1, \ldots, D_{m-1}$ and D_m.

Theorem 1[27] Suppose that there exists an f-connected family F with respect to $D_1, \ldots, D_{m-1}$ and D_m. Then there exists a compact invariant set $K \subset D$, such that $f|K$ is semi-conjugate to m-shift.

Here the semi-conjugacy is conventionally defined as follows. If there exists a continuous and onto map

$$h : K \to \Sigma_m,$$

such that $h \circ f = \sigma \circ h$, then f is said to be semi-conjugate to σ, where σ is the m shift (map) and Σ_m is the metric space of symbolic sequences to be defined below. Let $S_m = \{0, 1, \ldots, m-1\}$ be a set of non-negative successive integers from 0 to $m-1$. Let Σ_m be a collection of all bi-infinite sequences with their elements of Σ_m, i.e. $s \in \Sigma_m$ implies

$$s = \{\ldots, s_{-n}, \ldots, s_{-1}, s_0, s_1, \ldots, s_n, \ldots\},$$
$$s_i \in S_m \ \ \forall i.$$

Now consider another sequence $\bar{s} \in \Sigma_m$

$$\bar{s} = \{\ldots, \bar{s}_{-n}, \ldots, \bar{s}_{-1}, \bar{s}_0, \bar{s}_1, \ldots, \bar{s}_n, \ldots\}, \ \ \bar{s}_i \in S_m \ \ \forall i,$$

we define the distance between s and $\bar{s}$, denoted by $d(s, \bar{s})$, as follows:

$$d(s, \bar{s}) = \sum_{-\infty}^{\infty} \frac{1}{2^{|i|}} \frac{|s_i - \bar{s}_i|}{1 + |s_i - \bar{s}_i|}. \qquad (8)$$

With the distance defined as Eq. (8), Σ_m is a metric space, and the reader can refer to Ref. [28] for further explanation. The following result stated in Lemma 1 is an important fact.

Lemma 1 Consider two dynamical systems (X, f) and (Y, g). If (X, f) is semi-conjugate to (Y, g), then the topological entropy of f is not less than that of g, i.e.

$$\mathrm{ent}(f) \ge \mathrm{ent}(g).$$

In particular, if there exists a compact invariant set $K \subset D$, such that $f|K$ is semi-conjugate to the m shift σ, then

$$\mathrm{ent}(f) \ge \mathrm{ent}(\sigma) = \log m.$$

For the concept of topological entropy, the reader can refer to Ref. [29].

4.2. Horseshoe in system (2)

In this subsection, we will give the rigorous computer assisted verification of chaos in system (2).

We let $p = 1.99$; system (2) has the attractor as shown in Fig. 4 with initial point (1, 1, 1).

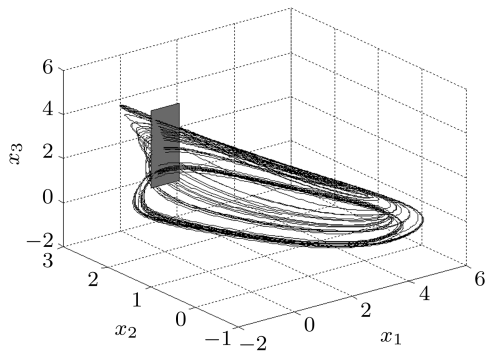


Fig. 4. The attractor of system (2) with parameter $p = 1.99$ and the cross section M.

Consider the cross section $M = \{(x_1, x_2, x_3) \in R^3 : x_2 = 1\}$, as shown in Fig. 4. The corresponding Poincaré map π is defined as follows:

$$\pi : M \to M.$$

For each point $x \in M$, $\pi(x)$ is the fourth return intersection point with M under the flow of system (2) with initial condition x. In this plane M, after a great many numerical simulations, we choose a subset of M to be the quadrangle $|ABCD|$ with its vertices being $A(-1.683,\ 1,\ 5.15)$, $B(-1.669,\ 1,\ 5.1)$, $C(-1.6695,\ 1,\ 4.9)$ and $D(-1.6835,\ 1,\ 4.95)$. Figure 5 is the quadrangle $|ABCD|$ and its image under the map π.

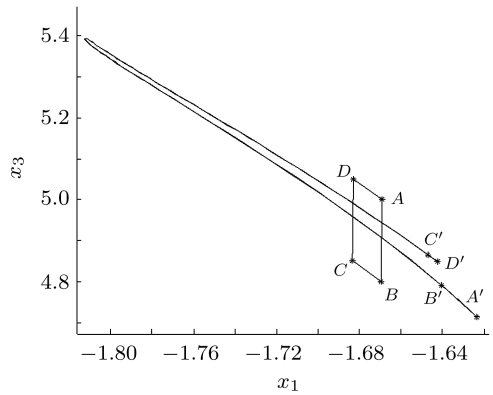


Fig. 5. The quadrangle $|ABCD|$ and its image under the map π.

Figures 5 indicates that under the map π, the quadrangle $|ABCD|$ is stretched and folded, and the image of $|ABCD|$ crosses the original quadrangle $|ABCD|$, which is evidence of the existence of a horseshoe.

Now we expect to find two subsets of $|ABCD|$, such that a π-connected family with respect to them exists. By a great deal of computer simulations, we find two subsets D_1 and D_2 of $|ABCD|$. The four vertices of D_1 are $G(-1.6705,\ 1,\ 5.1055)$, $A(-1.683,\ 1,\ 5.15)$, $B(-1.669,\ 1,\ 5.1)$ and $H(-1.6709,\ 1,\ 4.9050)$. The four vertices of D_2 are $D(-1.6835,\ 1,\ 4.95)$, $E(-1.6805,\ 1,\ 5.1410)$, $F(-1.6811,\ 1,\ 4.9415)$ and $C(-1.6695,\ 1,\ 4.9)$.

The subsets D_1 and D_2 of $|ABCD|$ are shown in Fig. 6. Under the Poincaré map π, D_1 and D_2 are mapped to D_1' and D_2'. Their vertices are mapped to A', B', C', D', E', F', G' and H' respectively. It is easy to see from Fig. 6 that D_1' and D_2' cross D_1 and D_2. That is to say, for every connection l with respect to D_1' and D_2', the images $\pi(l \cap D_1)$ and $\pi(l \cap D_2)$ lie wholly across the quadrangles D_1 and D_2. Then the images $\pi(l \cap D_1)$ and $\pi(l \cap D_2)$ are still connections with respect to D_1 and D_2. According to Definition 1 and Theorem 1, this means that the Poincaré map π is semi-conjugate to the 2-shift map. Hence, based on Lemma 1, we know that the entropy of the Poincaré map π is not less than $\log 2$, which means system (2) has positive topological entropy.

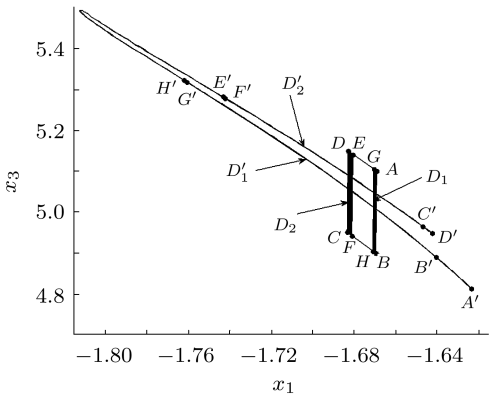


Fig. 6. Two disjointed compact subsets D_1, D_2 and their image D_1', D_2'.

5. Conclusion

In this paper, we have studied a simple 3D autonomous continuous time Hopfield neural network as described by system (2) with a parameter. In order to study the complex dynamical behaviours of the system, we have studied the Lyapunov exponent spectrum, phase portraits and bifurcation analysis. In particular, the system with one source and two saddle-foci

has a chaotic attractor and a periodic attractor with different initial points, which has rarely been reported in 3D autonomous systems. To confirm the chaos observed in system (2), we present rigorous computer-assisted verifications for the existence of a horseshoe in the system for a certain parameter.

References

[1] Lorenz E N 1963 *J. Atmos. Sci.* **20** 130
[2] Chen G R and Ueta T 1999 *Int. J. Bifur. Chaos* **9** 1465
[3] Lü J H and Chen G R 2002 *Int. J. Bifur. Chaos* **12** 659
[4] Lü J H, Chen G R, Cheng D Z and Celikovský S 2002 *Int. J. Bifur. Chaos* **12** 2917
[5] Chen Z Q, Qi G Y, Wang F Z and Yuan Z Z 2007 *Acta Phys. Sin.* **56** 3137 (in Chinese)
[6] Liu C X 2007 *Chin. Phys.* **16** 3279
[7] Liu C X and Wang F Q 2007 *Chin. Phys.* **16** 942
[8] Liu C X and Liu L 2009 *Chin. Phys.* B **18** 2188
[9] Qi G Y, Chen G R, Du S Z, Chen Z Q and Yuan Z Z 2005 *Physica* A **352** 295
[10] Qi G Y, Du S Z, Chen G R, Chen Z Q and Yuan Z Z 2005 *Chaos, Solitons and Fractals* **23** 1671
[11] Qi G Y, Chen G R and Zhang Y H 2008 *Chaos, Solitons and Fractals* **37** 409
[12] Qi G Y and Chen G R 2006 *Phys. Lett.* A **352** 386
[13] Chen Z Q, Qi G Y, Wang F Z, Yuan Z Z and Zhang Y H 2006 *Acta Phys. Sin.* **55** 4005 (in Chinese)
[14] Cang S J, Chen Z Q and Wu W J 2009 *Chin. Phys.* B **18** 1792
[15] Song Y Z, Zhao G Z and Qi D L 2006 *Chin. Phys.* **15** 2266
[16] Song Y Z 2007 *Chin. Phys.* **16** 1918
[17] Li W L and Song Y Z 2008 *Acta Phys. Sin.* **57** 51 (in Chinese)
[18] Liu C X and Xu Z 2008 *Chin. Phys.* B **17** 4033
[19] Liu L and Liu C X 2008 *Chin. Phys.* B **17** 2829
[20] Hopfield J J 1984 *Proc. Nat. Acad. Sci.* USA **81** 3088
[21] Aihara K, Takabe T and Toyoda M 1990 *Phys. Lett.* A **144** 333
[22] Bersini H 1998 *Neural Networks* **11** 1017
[23] Bersini H and Sener P 2002 *Neural Networks* **15** 1197
[24] Li Q, Yang X S and Yang F 2005 *Neurocomputing* **67** 275
[25] Yang X S and Yuan Q 2005 *Neurocomputing* **69** 232
[26] Yang X S and Huang Y 2006 *Chaos* **16** 033114
[27] Yang X S and Tang Y 2004 *Chaos, Solitons and Fractals* **19** 4
[28] Wiggins S 1990 *Introduction to Applied Nonlinear Dynamical Systems and Chaos* (New York: Springer-Verlag) p. 438
[29] Robinson C 1995 *Dynamical Systems: Stability, Symbolic Dynamics, and Chaos* (Florida: CRC Press)